Mon. Not. R. Astron. Soc. **000**, 1–?? (2013) Printed 23 February 2015 (MN LaTeX style file v2.2)

arXiv:1502.05824v1 [astro-ph.SR] 20 Feb 2015

Morphology and metallicity of the Small Magellanic Cloud using RRab stars

Sukanta Deb[1,2⋆], Harinder P. Singh[2] , Subhash Kumar[1,2], Shashi M. Kanbur[3]
[1] *Department of Physics, Acharya Narendra Dev College, Govindpuri, Kalkaji, New Delhi 110019, India*
[2] *Department of Physics & Astrophysics, University of Delhi, Delhi 110007, India*
[3] *State University of New York at Oswego, Oswego, NY 13126, USA*

Received on ; Accepted on

ABSTRACT

We present a study of three-dimensional structure of the Small Magellanic Cloud (SMC). The V- and I-band light curves of the fundamental mode RR Lyrae stars (RRab) obtained by the Optical Gravitational Lensing Experiment (OGLE)-III project were utilized in order to comprehend the SMC structure. The $[Fe/H]-P-\phi_{31}$ relation of Jurcsik & Kovacs (1996) is exploited to obtain the metallicities. From the three-dimensional RRab distance distributions, northeast (NE) arm and main body of the galaxy is identified. Combining metallicities with spatial distribution of these tracers, no radial metallicity gradient in the SMC has been detected. Dividing the entire sample into three parts: northeastern (NE), central and southwestern (SW), we find that the central part has a significantly larger line of sight depth as compared to rest of the parts, indicating that the SMC may have a bulge. Results obtained from the I-band data seem to be reliable and were further substantiated using the Smolec (2005) relation. Distribution of SMC RRab stars were modeled as a tri-axial ellipsoid. Errors in structural parameters of the SMC ellipsoid were obtained from Monte Carlo simulations. We estimated the axes ratios of the galaxy as $1.00 \pm 0.000 : 1.310 \pm 0.029 : 8.269 \pm 0.934$, the inclination of the longest axis with line of sight $i = 2^\circ.265 \pm 0^\circ.784$, and the position angle of the line of nodes $\theta_{\rm lon} = 74^\circ.307 \pm 0^\circ.509$ from the variance weighted I-band determinations.

Key words: stars: variables: RR Lyrae-stars:fundamental parameters - stars: Population II - galaxies: statistics - galaxies:structure - galaxies:Magellanic Clouds

1 INTRODUCTION

The Small Magellanic Cloud (SMC) is one of our nearby satellite galaxies. It is a gas-rich, dwarf irregular galaxy connected by a hydrogen gas and stellar bridge to the Large Magellanic Cloud (LMC) and located at a distance of around 60 kpc (Westerlund 1997; Graczyk et al. 2014). Like LMC, the SMC also exhibits a bar which is less pronounced (Westerlund 1997; Subramanian & Subramaniam 2012). The complexity in the structure, dynamics and evolution of the SMC might be attributed to the influence of gravitational interactions with the LMC and the Galaxy (Putman et al. 1998). The SMC has a relatively lower heavy metal abundance, lower dust content and significantly larger line of sight depth as compared to the LMC and the Galaxy (Stanimirovic et al. 1999; Stanimirović et al. 2004; Subramanian & Subramaniam 2012). With the proliferation of accurate and precise variable star data generated from modern astronomical surveys and space missions along with their well-established theoretical understandings have helped us to gain better knowledge about distances of astronomical objects and resolved many issues related to distances and distance related parameters such as Galactic and extragalactic structures (Subramanian & Subramaniam 2012; Kapakos & Hatzidimitriou 2012; Pietrzyski et al. 2013; Graczyk et al. 2014). For instance, to gain a better knowledge of the geometric structure of the SMC, Graczyk et al. (2014) determined the distance to the SMC as $(m-M) = 18.965 \pm 0.025(\text{stat.}) \pm 0.048(\text{sys.})$ mag which corresponds to a distance of 62.1 ± 1.9 kpc using detached, long period eclipsing binaries. Well-detached eclipsing binaries serve as a source of accurate and precise distance indicators and help in the calibration of the zero point of the cosmic distance scale with an accuracy of about 2% (Pietrzyski et al. 2013).

The long-standing and highly controversial questions

⋆ E-mail: sukantodeb@gmail.com

of the SMC's three-dimensional structure and depth along the line of sight have been greatly facilitated through the identification and characterization of a statistically significant number of different stellar tracers in various large photometric surveys. The uniform data sets obtained for a large number of different stellar tracers obtained in these surveys in the SMC provide a unique opportunity to study the characteristics of the host galaxy to a great detail (Subramanian & Subramaniam 2012; Kapakos & Hatzidimitriou 2012; Subramanian & Subramaniam 2014).

The accurate determination of the geometrical parameters of the SMC plays an important role in modeling the interactions between the galaxy, LMC and the SMC. In this study, the 'standard candles' such as the RRab stars have been chosen to study the various parameters of the SMC. RRab stars are the RR Lyrae stars which pulsate in the fundamental mode. RR Lyrae stars are metal-poor, low-mass and core-helium burning stars that undergo periodic radial pulsations (Smith 2004). They serve as excellent tracers of the oldest population of stars in a host galaxy. Their constant mean luminosity makes them ideal standard candles (Pritzl et al. 2011). They serve as invaluable resource which help in exploring the metallicity and structure and hence provide substantial insight into the understanding of the formation and evolution of the galaxy (Parisi et al. 2009; Deb & Singh 2014). They have been used as proxies of the true, three-dimensional spatial distribution of host galaxies. Their presence in large numbers in different galaxies has led to an improved understanding of various geometric parameters of these galaxies. Well-sampled light curves covering the entire pulsational period of the RRL stars allow determination of their properties with high precision. The derived structural parameters extracted from their light curves can be used to determine metallicity, interstellar extinction, distance and spatial distribution of the stars (Pietrzynski et al. 2012).

There are a few studies in the literature aimed at determining the geometrical structure of the SMC (Stanimirovic et al. 1999; Crowl et al. 2001; Subramanian & Subramaniam 2012; Kapakos & Hatzidimitriou 2012; Haschke et al. 2012; Subramanian & Subramaniam 2014). Investigating 12 populous clusters in the SMC, Crowl et al. (2001) determined the axes ratios approximately as 1 : 2 : 4 modeling the SMC as a triaxial galaxy with declination, right ascension and line of sight depth as the three axes. Using the red clump and RR Lyrae stars in the V and I-band data taken from OGLE-III, Subramanian & Subramaniam (2012) derived various geometrical parameters of the SMC. Their study was based on the relative position of different regions of the SMC with respect to the SMC mean distance. The parameter determinations of the SMC in their work do not quote the errors. It is to be noted that the geometry of the SMC is a function of the de-projected Cartesian coordinates as well as their errors. Accurate parameter values can only be determined when the errors are incorporated in projected Cartesian coordinates along with the reliable distance determinations. Also, the metallicity determination of the RR Lyrae stars were not attempted in their work which is very crucial in understanding of substructure of the galaxy. The axes ratios, inclination angle of the longest axes along the line of sight (i) and position angle of the line of nodes (θ_{lon}) obtained by Subramanian & Subramaniam (2012) from the distribution of the SMC RR Lyraes were found to be 1 : 1.33 : 6.47, $0^\circ.4$ and $74^\circ.4$, respectively from the entire dataset. Taking different coverage of the dataset and removing the isolated northwestern fields, different structural parameters of the SMC ellipsoid were also attempted and estimated by Subramanian & Subramaniam (2012). On the other hand, using the 454 OGLE-III RRab data in the V-band, Kapakos & Hatzidimitriou (2012) used the line of sight distances and the metallicity values to investigate the possible presence of different structures containing different populations in the SMC. Using spherical shells of different radii of 2.5, 3.0 and 3.5 kpc, they obtained the axes ratios of the SMC ellipsoid as: 1 : 1.21 : 1.57, 1 : 1.18 : 1.53 and 1 : 1.23 : 1.80, respectively, whereas, inclination angle and position angle of line of nodes of the SMC were not calculated in their analyses. From an analysis of radial velocities of 150 carbon stars, Kunkel et al. (2000) estimated the inclination of the SMC orbital plane to be $i = 73^\circ \pm 4^\circ$ relative to the plane of the sky. Using Cepheids, Caldwell & Coulson (1986) and Groenewegen (2000) estimated i as $70^\circ \pm 3^\circ$ and $68^\circ \pm 2^\circ$, respectively. The position angle of line of nodes was estimated to be $\sim 148^\circ$ (Groenewegen 2000). Estimates of inclination angle and position angle of line of nodes obtained by Haschke et al. (2012) from the I-band OGLE III SMC RRab data are $7^\circ \pm 15^\circ$ and $83^\circ \pm 21^\circ$, respectively. From the study of distance distribution of Cepheids in the SMC using the OGLE-III data, Haschke et al. (2012) found that these young populations are differently oriented than the old population RR Lyrae stars. The inclination angle and position angle parameters of the SMC obtained from Cepheids by Haschke et al. (2012) are $74^\circ \pm 9^\circ$ and $66^\circ \pm 15^\circ$, respectively. Other recent estimates of inclination angle and position angle of lines of nodes for the SMC obtained from Cepheids are $64^\circ.4 \pm 0^\circ.7$ and $155^\circ.3 \pm 6^\circ.3$, respectively (Subramanian & Subramaniam 2014).

In this paper, we use available V and I-band OGLE-III data in order to determine the absolute magnitudes and metallicities of RRab stars. These measurements along with equatorial coordinates, viz., right ascension (α) and declination (δ) have been utilized to get an insight into the understanding of the three-dimensional structure of the SMC and its metallicity distribution. The availability of data in two different bands and the use of different methodologies of distance determinations provide a unique opportunity to compare and contrast various structural parameter determinations. The roadmap of the present investigation is to use these tracers for the distance determinations and obtain distances relative to the center of the SMC. The principal axis transformation method as described in Deb & Singh (2014) was used to get the viewing angle and geometrical parameters of the galaxy. Section 2 describes the data used for the analysis in the present study. Fourier decomposition method and sample selection criteria are described in section 3. Section 4 focusses on extinction measurements for the OGLE-III data along the line of sight using the SMC extinction map from Zaritsky (1999); Zaritsky et al. (2002). Determination of metallicities (Jurcsik & Kovacs 1996) and absolute magnitudes (Kovács & Walker 2001; Catelan & Cortés 2008) from V-band and I-band data calibrated to the V-

band are described in section 5. Viewing angle parameters and geometrical parameters of the SMC determined for the above dataset are described in section 6. Line of sight depth and existence of metallicity gradient are examined in sections 7 and 8, respectively. Results obtained from the above analyses were further substantiated as described in section 9 with Smolec (2005) metallicity relation using the I-band light curve data and exploiting the $M_V - [Fe/H]$ relation of Catelan & Cortés (2008). Exponential disk model and King (1962) three parameter model for the radial number density distribution of RRab stars in the I-band are discussed in section 10. Lastly, summary and discussions of the present investigation are laid down in section 11.

2 THE DATA

RRab stars for the present study were selected from OGLE-III catalog of variable stars that consists of 8-year archival data identified and characterized by the Fourier coefficients of the light curves (Soszyński et al. 2009). The catalog comprises 1933 RRab stars in the I-band having a mean period of $< P_{ab} >= 0.596$ days with typical accuracy of $\sigma_P/P \simeq 10^{-5}$ (Soszyński et al. 2009). The catalog is based on the observations carried out at the Las campanas Observatory, Chile with a 1.3-m telescope. The time series observations of the SMC consist of 800 nights between June 2001 and May 2009. The OGLE field in the SMC covers nearly 16 deg^2 covering the bar and the wing. Most of the observations were carried out using the Cousins I-band filter with exposure time of 180 s having an average of 400 photometric observations. The catalog also contains V-band light curves of 1887 stars having an average of 30 data points per light curve with the exposure time of 225 s (Soszyński et al. 2009).

3 FOURIER DECOMPOSITION METHOD AND SAMPLE SELECTION

The Fourier decomposition method was used to obtain V and I-band light curve parameters of the SMC RRab stars. The light curves were fitted with a Fourier sine series of the form (Deb & Singh 2009, 2010, 2014)

$$m(t) = A_0 + \sum_{i=1}^{N} A_i \sin\left[i\omega(t-t_0) + \phi_i\right], \qquad (1)$$

where $m(t)$ is the observed magnitude, A_0 is the mean magnitude, ω=$2\pi/P$ is the angular frequency, P is the pulsational period of the star in days and t is the time of observation. t_0 represents the epoch of maximum light (either in the V or the I-band) and is used to obtain a phased light curve which has maximum light at phase zero. A_i's and ϕ_i's are the ith order Fourier coefficients and N is the order of the fit. Eqn. 1 has $2N+1$ unknown parameters. To solve for these parameters, at least the same number of data points are required. The light curve phase was obtained using

$$\Phi = \frac{(t-t_0)}{P} - Int\left(\frac{(t-t_0)}{P}\right).$$

Here $\Phi \in [0,1]$ represents one pulsation cycle of the RRab stars. The pulsation periods (P) and the epoch (t_0) are taken from the OGLE catalog. The Fourier parameter code as described in Deb & Singh (2010) was used to obtain various Fourier parameters on the right hand side of Eqn. 1. Fifth order and seventh order Fourier fits were employed to model the RRab V and I-band light curves, respectively. The Fourier fitted V and I-band light curves of a sample of RRab stars are shown in Fig. 1. The phase differences, $\phi_{i1} = \phi_i - i\phi_1$ and amplitude ratios, $R_{i1} = (A_i/A_1)$, $i > 1$ were evaluated and standard errors were determined using the formulae of Deb & Singh (2010). A clean sample of RRab stars for the present analysis were selected with the criteria based on OGLE-determined periods, the mean magnitude (A_0) and the peak-to-peak V and I-band amplitude (A_V, A_I) determined from the Fourier analysis of the phased light curves. RRab stars with periods $P \geqslant 0.4$ days, mean magnitude $A_0 \geqslant 18.0$ mag (I-band)and amplitude $0.1 \leqslant A_I \leqslant 1.2$ mag were chosen for the I-band light curves. On the other hand, to select the V-band light curves, the same criteria on periods has been applied. While the following criteria were applied on A_0 and amplitude: $A_0 \geqslant 18.5$ mag (V-band) and amplitude $0.2 \leqslant A_V \leqslant 1.5$. These selection criteria were applied in order to collect a clean sample of RRab stars of the SMC which are free from any contamination due to the foreground objects of our Galaxy and the LMC. The application of these selection criteria along with further application of compatibility test of Jurcsik & Kovacs (1996) reduces the number of RRab stars in the V and I-band light curves to 1142 and 1543, respectively for the physical parameter estimation and determination of structure of the SMC. The compatibility test of Jurcsik & Kovacs (1996) ensures to reject those RRab stars that have deviation parameter values $D_F > 5$.

4 INTERSTELLAR EXTINCTION

Interstellar medium plays an important role in dimming and reddening of the star light. In order to determine accurate distances to stars, interstellar reddening must be accounted for. Various methods to determine interstellar extinction exist in the literature using different tracers. Observations of multiband photometry available for RR Lyrae stars serve to resolve internal extinction in the case of host galaxy (Pejcha & Stanek 2009). For the determination of interstellar extinction in the case of individual RRab stars in this paper, we adopted the Zaritsky (1999); Zaritsky et al. (2002, hereafter, Zaritsky map) extinction map for the SMC which comes in FITS (Flexible Image Transport System) format. The SMC extinction map for cool stars is downloaded from [1], since the cool star data are characteristics of the RR Lyrae with $T_{\rm eff} \sim 6500$ K. The Magellanic Cloud Photometric Survey (MCPS) contains $UBVI$ photometry and extinction map for the central 18 deg^2 area of the SMC (Zaritsky et al. 2002). For a given RRab location, the map returns the V-band extinction value, A_V. The FITS image of the Zaritsky map containing the extinction values (A_v) is an array of (240×280) pixels with reference pixel coordinate as $(X,Y) = (120,140)$ corresponding to the $(RA, DEC) = (12^\circ.750, -72^\circ.699)$. The RA and DEC pixel

---

[1] `http://djuma.as.arizona.edu/~dennis/mcsurvey/Data_Products.html`

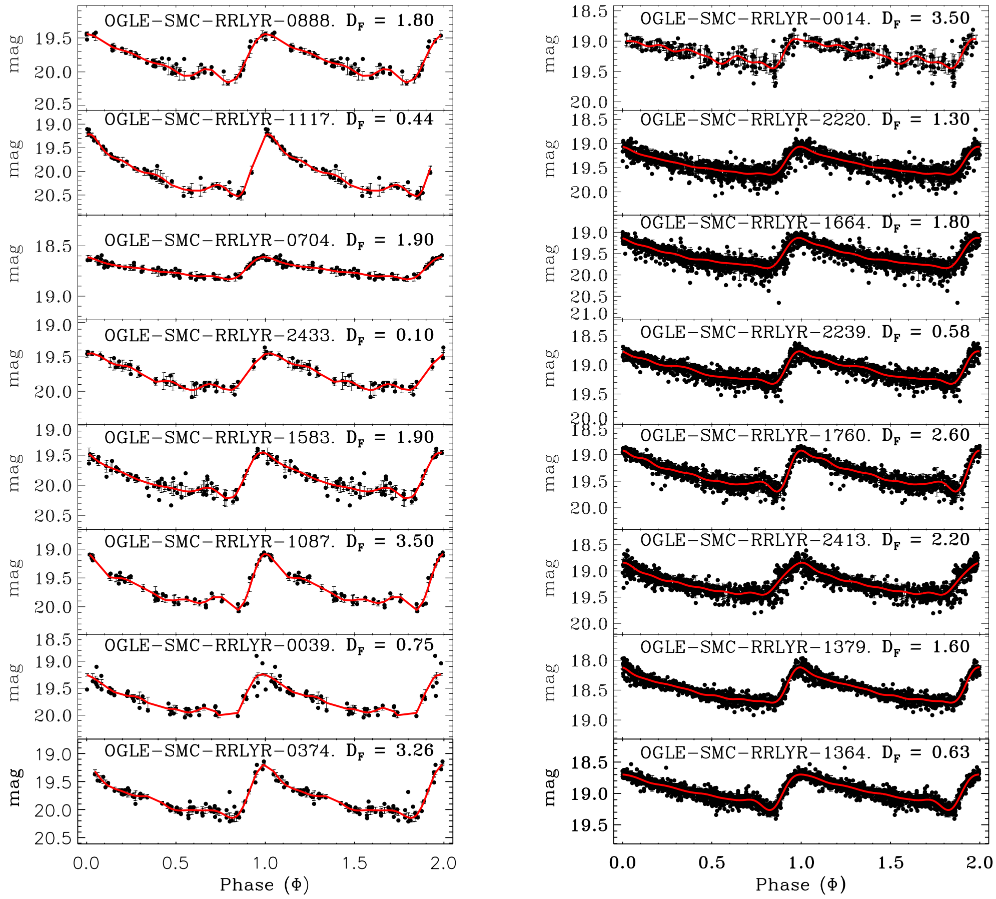

Figure 1. A collection of randomly selected sample of RRab light curves with their corresponding OGLE IDs and deviation parameters (D_F) are shown. Left panel shows the phased light curve data in V-band while the right panel depicts the same in the I-band.

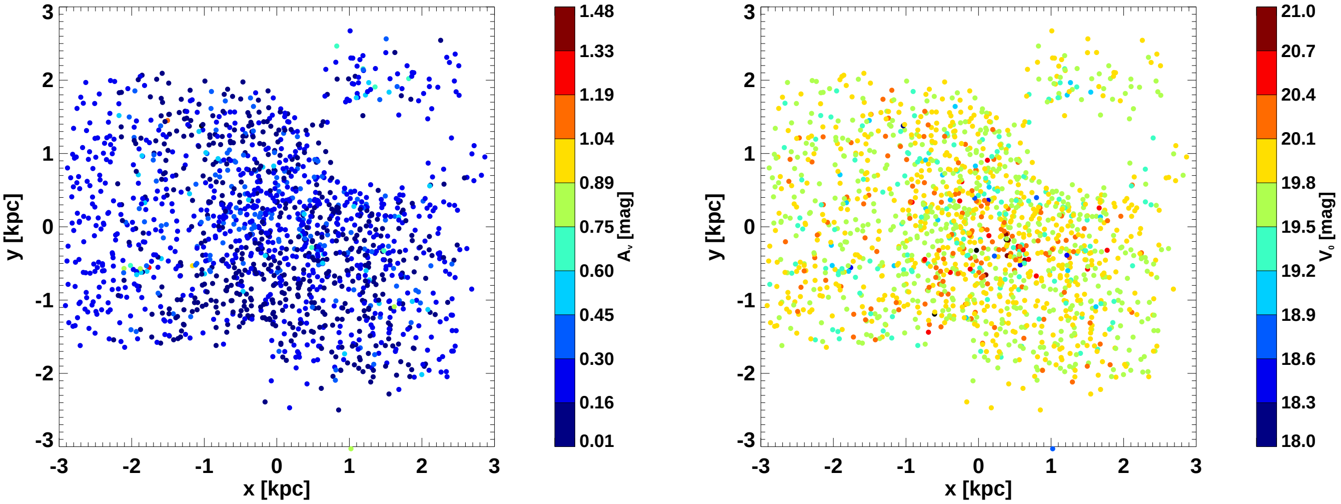

Figure 2. Two-dimensional color bar plot of the interstellar extinction values (A_V) and extinction corrected mean magnitudes (V_0) of RRab stars.

scales in the image are $\sim 0.0167^\circ$/pixel which correspond to $1'$/pixel. The IRAF task 'imhead' was used to get the details of the FITS image header. The number of stars used to derive extinction for map pixels were at least 3 where the median extinction value was adopted (Zaritsky 1999). The Zaritsky map has regions of high and low spatial resolution but relatively uniform signal-to-noise ratio. The details of smoothing algorithm applied to derive the extinction values for the map pixels are outlined in Zaritsky (1999). The following procedure was adopted to get the extinction values of the sample of RRab stars. RA(α) and Dec(δ) of the sample stars were first converted into X/Y pixel coordinates using *sky*2*xy* followed by running *getpix* on the FITS image to get interstellar extinction (A_V) at that X/Y position. Both *sky*2*xy* and *getpix* are the codes from WCSTOOLS [2]. For a few stars, we get a null value of A_V. For these stars, the mean value of $A_V = 0.155$ mag appropriate for the SMC was used. The average value of A_V for the OGLE-III RRab's is 0.155 ± 0.127 mag which translates into a mean $E(B-V)$ of 0.048 ± 0.039 mag. This is comparable to the mean $E(B-V)$ value of 0.054 mag and $E(V-I)$ value of 0.07 ± 0.06 mag, respectively by Caldwell & Coulson (1985) obtained from the analysis of 48 Cepheids and Haschke et al. (2011) from the analysis of 1529 SMC RRab stars. Since no formal errors are given by the map for the individual stars, an error margin of 20% is assumed in the individual extinction values if these estimates from the map are taken to be reliable. The extinction maps derived from the OGLE RRab stars by Haschke et al. (2011, hereafter, Haschke map) were found to be in good agreement with those obtained from the Zaritsky reddening map. Fig. 2 depicts two-dimensional color bar plot of interstelar extinction values (A_V) and extinction corrected mean magnitudes (V_0) of RRab stars. x and y in the figure denote projected Cartesian coordinates.

5 METALLICITIES AND ABSOLUTE MAGNITUDES

Metallicities of a large number of stars found in a certain galaxy play pivotal role in understanding the formation of various structures of that galaxy. Assembly of stars having certain metallicity ranges concentrated in a particular part of a galaxy tells the epoch of its formation. Although the metallicity is an important parameter for understanding chemical properties of the underlying stars and hence that of the distant host galaxy and its formation, it is hard and time-consuming to obtain the metallicity spectroscopically for a large number of stars. Calibrated relationships between various photometric light curve parameters and spectroscopic metallicities of RRab stars provide efficient and robust ways for determining the metallicities in various globular clusters, the Galaxy, the SMC and the LMC by recent ground-based automated surveys. Previous studies have shown that metallicities of RRab stars can be derived from an empirical relation connecting spectroscopic metallicities and the light curve parameters as proxies (Simon 1988; Jurcsik & Kovacs 1996; Sandage 2004; Nemec et al. 2013). These studies have shown that metalicities of RRab stars can be linked the period with some intermediate parameters such as amplitude (A), Fourier phase parameters ϕ_{21}, ϕ_{31} (Jurcsik & Kovacs 1996; Alcock et al. 2000; Sandage 2004; Nemec et al. 2013). The correlation between the light curve structures of RR Lyrae stars such as the period (P), Fourier coefficients (ϕ_{21}, ϕ_{31}) and their metallicities was first noticed and studied in the pioneering work by Simon (1988). This work has motivated many investigators such as Jurcsik & Kovacs (1996) and his collaborators, Sandage (2004) to derive semi-empirical relations involving light curve structures and spectroscopically determined metallicities.

The unprecedented amount of photometric light curve data generated from the recent automated surveys such as OGLE, ASAS (All Sky Automated Survey), and highly accurate and precise stellar data obtained from the NASA's *Kepler* mission have provided a new avenue into the understanding of various astrophysical problems more accurately. Although the $[Fe/H]-P-\phi_{31}$ relation of Jurcsik & Kovacs (1996) is widely used in the determination of metallcities of RR Lyrae stars from their photometric light curves, accurate light curve data of these stars generated from the NASA's *Kepler* mission have helped in refining the model parameters of existing $[Fe/H]-P-\phi_{31}$ relation and calibrate new relations based on the new data (Nemec et al. 2013). These relations will prove to improve our knowledge in understanding the chemical history of the stellar tracers as well as structure of the host galaxy from their distance distributions. Metallicities $[Fe/H]_{\rm spec}$ of the corresponding light curves in Nemec et al. (2013) were obtained from the high resolution spectroscopic measurements.The empirical relation of Jurcsik & Kovacs (1996) connecting ϕ_{31} in the V- band, period P and the metallicity $[Fe/H]$ is given by

$$[Fe/H]_{JK} = -5.038 - 5.394\,P + 1.345\,\phi_{31}, \quad \sigma = 0.14. \quad (2)$$

On the other hand, the non-linear relation connecting $P - \phi_{31} - [Fe/H]$ using 26 RRab stars obtained by the NASA's *Kepler* space telescope in the K_p-band is given by (Nemec et al. 2013)

$$[Fe/H]_{\rm N13} = (-8.65 \pm 4.64) + (-40.12 \pm 5.18)P + (5.97 \pm 1.72)P\phi^s_{31} + (6.27 \pm 0.96)(\phi^s_{31})^2, \quad \sigma = 0.084 \quad (3)$$

where ϕ^s_{31} is the mean $\phi^s_{31}(Kp)$ value and $[Fe/H]$ is the spectroscopic metallicity value obtained from the recent new high resolution spectroscopic measurements (Nemec et al. 2013). In order to apply the N13 relation to the V-band data, Nemec et al. (2011) gave the following inter-relation

$$\phi^s_{31}(V) = \phi^s_{31}(Kp) - (0.151 \pm 0.026). \quad (4)$$

The above inter-relation was derived by Nemec et al. (2013) using the ASAS V-band and the Kepler photometric light curve based on only 3 stars. The inter-relation was recently refined using V band photometric data of 34 common stars in the Kepler field and the following relation was obtained (Jeon et al. 2014)

$$\phi^s_{31}(V) = \phi^s_{31}(Kp) - (0.174 \pm 0.085). \quad (5)$$

In the present analysis, we have determined metallicities using Jurcsik & Kovacs (1996) linear relation. Although the Nemec et al. (2013) relation is based on the highly accurate and precise *Kepler* data, we have found from numerical analysis that formal errors on the calculated $[Fe/H]$ values

---

[2] `http://tdc-www.harvard.edu/wcstools/`

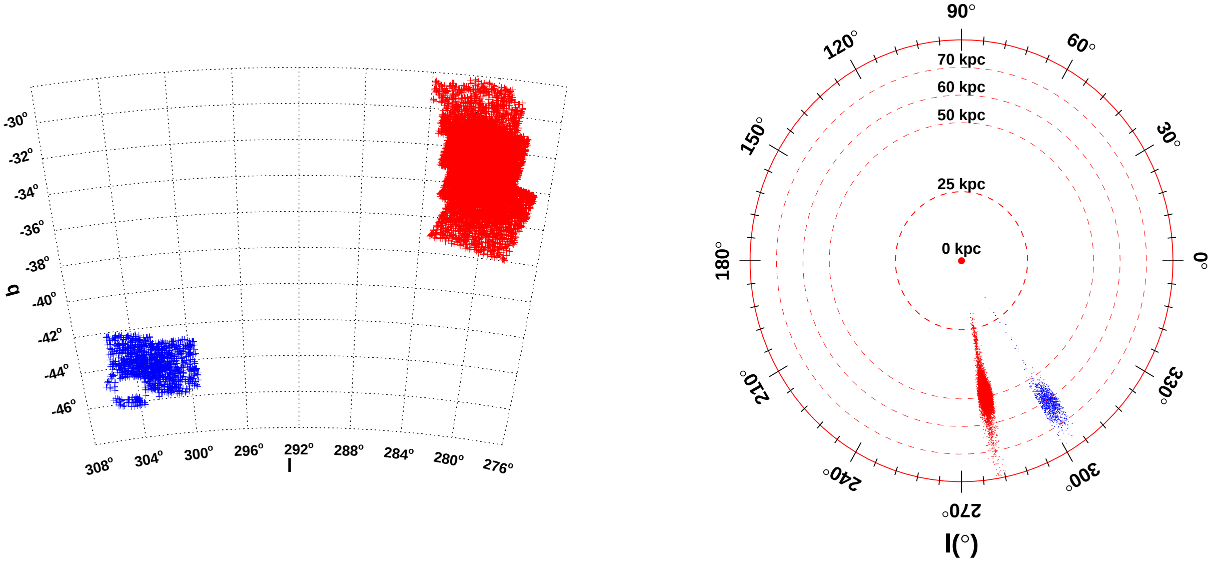

Figure 3. Left panel shows LMC and SMC RRab stars in galactic coordinates (l, b). Right panel depicts polar plot of distance distribution of LMC and SMC RRab stars in galactic coordinates (l, b). The dashed lines are set at distances $D = 25, 50, 60, 70$ kpc, respectively. LMC and SMC stars are shown as red and blue data points, respectively. LMC RRab stars are taken from Deb & Singh (2014). The tails of distance distributions of the two Magellanic Clouds account for possible contaminations from the foreground and background RRab stars.

from the derived relation turn out to be very large using the propagation of error formula of Bevington & Robinson (2003). This might be attributed to the larger errors in ϕ_{31} values for the OGLE-III data and more number of complexity parameters of the derived relation. Hence because of limitations of the relation restricted to highly accurate dataset, we have to leave out using the Nemec et al. (2013) relation for the OGLE-III dataset. The absolute magnitudes are determined using the following relation (Catelan & Cortés 2008)

$$M_V = (0.23 \pm 0.04)[Fe/H] + (0.984 \pm 0.127), \qquad (6)$$

where $[Fe/H]$ is the metallicity in the Zinn & West (1984) scale. The metallicity values obtained from Eqn. 2 are in Jurcsik & Kovacs (1996) scale, which can be transformed into the metallicity scale of Zinn & West (1984) using the relation from Jurcsik (1995):

$$[Fe/H] = \frac{[Fe/H]_{JK} - 0.88}{1.431}. \qquad (7)$$

Determination of absolute magnitudes of the present sample of RRab stars using Eqn. 6 is denoted as 'MVC'. The absolute magnitudes of the selected samples of RRab stars were also determined using the following empirical relation in terms of the period (P) and the Fourier coefficients (A_1 and A_3) (Kovács & Walker 2001; Arellano Ferro et al. 2010):

$$M_V = -1.876 \log P - 1.158 A_1 + 0.821 A_3 + 0.41. \qquad (8)$$

Absolute magnitude determination using this relation is referred to as 'MVF'. Both the methods of absolute magnitude determination were applied in V and I-band to calculate distances of the present sample of RRab stars. Suitable inter-relations between the Fourier parameters in the V and I-band were utilized as discussed in Deb & Singh (2010, 2014). Geometrical parameter determinations of the SMC using two different relations in two different bands carried out in this paper will help us in improving their estimates. Fig. 3 shows polar plot of distance distribution of the SMC RRab stars (I-band calibrated to V-band) in galactic (l, b) coordinates. LMC RRab stars as in Deb & Singh (2014) are also overplotted. The two-dimensional density contours of the distribution of the LMC RRab stars taken from Deb & Singh (2014) and the SMC RRab stars in the present study are shown in Fig. 4. The star symbol denotes the location of the centroid of the present sample. Two-dimensional color bar plot of distance distributions of SMC RRab stars is shown in Fig. 5.

6 STRUCTURE OF THE SMC

Availability of a statistically significant sample of RRab stars from the OGLE-III data in I and V-band provides an opportunity to compare and contrast the two different bands to geometric parameter determination of the SMC. Furthermore, structural parameter determinations of the SMC substantiated using two independent distance determination formula will also help us in improving the structural parameters of the SMC. In order to determine the structure, we have converted the right ascension (α), declination (δ) and the distance (D) into the corresponding Cartesian coordinates (x, y, z). Let us consider the Cartesian coordinate system (x, y, z) which has the origin in the center of the SMC at $(\alpha, \delta, D) = (\alpha_0, \delta_0, D_0)$. The z axis is pointed towards the observer. x-axis is antiparallel to the α-axis, the y-axis is parallel to the δ-axis. D_0 is the distance between the center of the SMC and the observer.

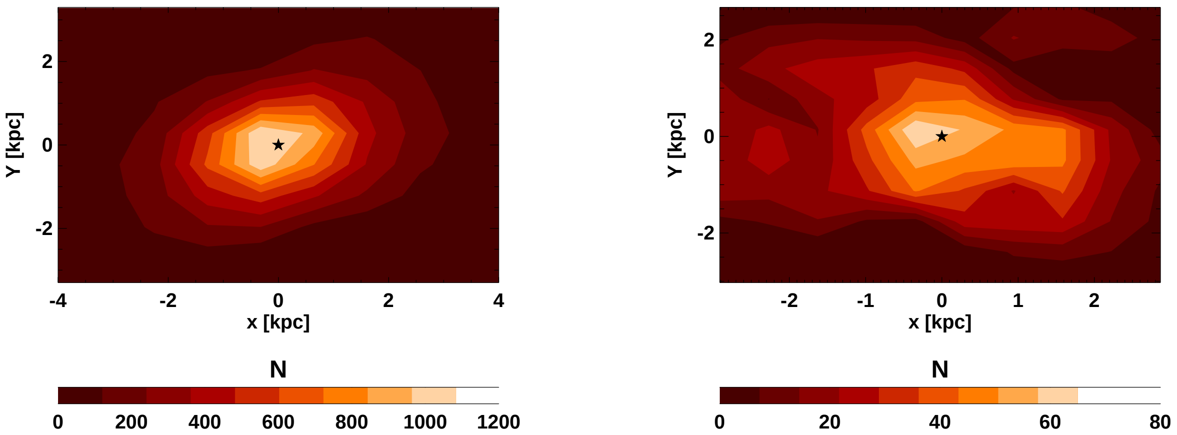

Figure 4. Left panel shows two-dimensional density contours of the LMC RRab stars taken from Deb & Singh (2014). Right panel shows the same for the SMC RRab stars in the present study. The star symbol denotes the location of the centroid.

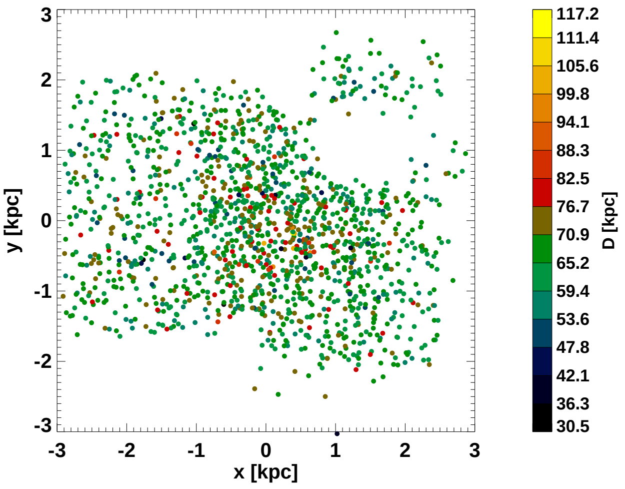

Figure 5. Two-dimensional color bar plot of distance distribution of SMC RRab stars as a funtion of (x, y) coordinates.

D is the observer-source distance. (α_0, δ_0) are the equitorial coordinates of the center of the SMC. The center of the SMC is taken as $(\alpha_0, \delta_0) = (0^{\mathrm{h}}53^{\mathrm{m}}31^{\mathrm{s}}, -72^{\circ}59'15''.7)$ (Subramanian & Subramaniam 2012). The (x, y, z) coordinates are obtained using the transformation equations (van der Marel & Cioni 2001; Weinberg & Nikolaev 2001):

$$x = -D\sin(\alpha - \alpha_0)\cos\delta,$$

$$y = D\sin\delta\cos\delta_0 - D\sin\delta_0\cos(\alpha - \alpha_0)\cos\delta,$$

$$z = D_0 - D\sin\delta\sin\delta_0 - D\cos\delta_0\cos\alpha - \alpha_0\cos\delta.$$

The coordinate system of the SMC disk (x', y', z') is the same as the orthogonal system (x, y, z), except that it is rotated around the z-axis by the position angle θ counterclockwise and around the new x-axis by the inclination angle i clockwise. The coordinate transformations are (van der Marel & Cioni 2001; Weinberg & Nikolaev 2001):

$$\begin{bmatrix} x' \\ y' \\ z' \end{bmatrix} = \begin{bmatrix} \cos\theta & \sin\theta & 0 \\ -\sin\theta\cos i & \cos\theta\cos i & -\sin i \\ -\sin\theta\sin i & \cos\theta\sin i & \cos i \end{bmatrix} \begin{bmatrix} x \\ y \\ z \end{bmatrix}$$

The errors $(\sigma_x, \sigma_y, \sigma_x)$ in the Cartesian coordinates were obtained following the propagation of error formula (Bevington & Robinson 2003). Observed distribution of RRab stars in the SMC was modeled by a triaxial ellipsoid. Properties of the ellipsoid are obtained from the moment of inertia tensor using the principal axes transformation method (Deb & Singh 2014). The axes ratios $\frac{S_i}{S_0}$, where $i = 0, 1, 2$, inclination of the longest axis along the line of sight (i), position angle of line of nodes (θ_{lon}) along with their associated errors were calculated using the Monte Carlo simulations. The Monte Carlo simulations for finding errors in the geometrical parameters were obtained with the assumption that the probability distribution of errors in the parameters are Gaussian and the errors in the obtained (x, y, z) values are reliable. The observed projected Cartesian coordinates (x, y, z) were simulated with the following steps:

(1) The observed Cartesian coordinates (r_i, σ_{r_i}) were obtained from the transformations connecting them with the given $(\alpha_i, \delta_i, D_i)$ along with the application of propagation of error formulae (Bevington & Robinson 2003), where $r_i = (x_i, y_i, z_i)$ and $\sigma_{r_i} = (\sigma_{x_i}, \sigma_{y_i}, \sigma_{z_i})$. $i = 1, 2, \ldots, N$ and N is the number of data points.

(2) r_i's were taken as the centroid of the Gaussian.

(3) Box-Muller method was then used to get Gaussian distributed points having σ_{r_i}'s as errors and r_i's as centroids. Essentially, this consists of the following steps (Bevington & Robinson 2003):

$$r_i = r_i + \sigma_{r_i} k_i,$$

with $k_i = \sqrt{-2.0\log(u_i)}\cos(2.0\pi v_i)$, where (u_i, v_i) are pairs of uniformly distributed random numbers.

Principal axis transformation method as described in Deb & Singh (2014) was then applied to the simulated Cartesian coordinates of the SMC RRab stars to obtain viewing angles and other geometric parameters of the galaxy. The Monte Carlo simulation was carried for 10^5 steps and corresponding values of the parameters were determined in each iteration. The distribution of various geometric parameters were then obtained after binning with a proper binsize. Distribution of the geometric parameters were found to be Gaussian. Hence, three parameter Gaussian fitting was applied to the histogram distributions. The σ values of the fitted Gaussian distributions were taken as errors in various parameters. Viewing angle parameters $(i, \theta_{\rm lon})$ and geometrical parameters such as axes ratios $(S_0/\overline{S_0}, S_1/S_0, S_2/S_0)$ described in Deb & Singh (2014) obtained from the entire dataset of SMC RRab stars are shown in Figs. 6 and 7. Their values are listed in Table 1.

From the Cartesian three-dimensional distribution of RRab stars as shown in Fig. 8, it is quite evident that north east (NE) arm is nearer to us than the SMC main body. In order to find exact location of NE arm of the SMC, we have used an R[3] statistical package *changepoint* for changepoint analysis (Killick & Eckley 2014; Killick et al. 2014). The function cpt.meanvar() was used to find changes in the mean and variance for z distribution. Locations of main body and NE arm of the SMC were thus identified from the changepoint analysis. Principal axis transformation method was then applied to the SMC main body since its distribution resembles a three-dimensional ellipsoid. This is done in four cases (Two in each bands corresponding to the methods 'MVF' and 'MVC'). Results obtained from the principal axis transformation method are shown in Table 2. On the other hand, NE arm of the SMC resembles like a plane. Therefore, plane-fitting procedure was applied to find its viewing angle parameters such as inclination and position angle of line of nodes. NE arm of the SMC was fitted with a plane-fitting equation of the form (Nikolaev et al. 2004)

$$z_i = c + a x_i + b y_i, \; i = 1, 2, \ldots, N, \tag{9}$$

where N is the number of data points. The inclination angle $(i[^\circ])$ can be obtained from

$$i = \arccos\left(\frac{1}{\sqrt{(1 + a^2 + b^2)}}\right),$$

and if we define $\gamma = \arctan(|a|/|b|)$, then

$$\theta_{\rm lon} = \begin{cases} \gamma & \text{if } \; a < 0 \; \text{ and } \; b > 0, \\ \gamma & \text{if } \; a > 0 \; \text{ and } \; b < 0, \\ \frac{\pi}{2} + \gamma & \text{if } \; a < 0 \; \text{ and } \; b < 0, \\ \frac{\pi}{2} + \gamma & \text{if } \; a > 0 \; \text{ and } \; b > 0, \\ 0 & \text{if } \; a = 0 \; \text{ and } \; b \neq 0, \\ \text{sign}(a)\frac{\pi}{2} & \text{if } \; a \neq 0 \; \text{ and } \; b = 0, \\ \text{undef.} & \text{if } \; a = b = 0. \end{cases}$$

A weighted plane-fitting procedure using mpfitfun in IDL was used to fit NE arm of the SMC (Markwardt 2009, 2012).

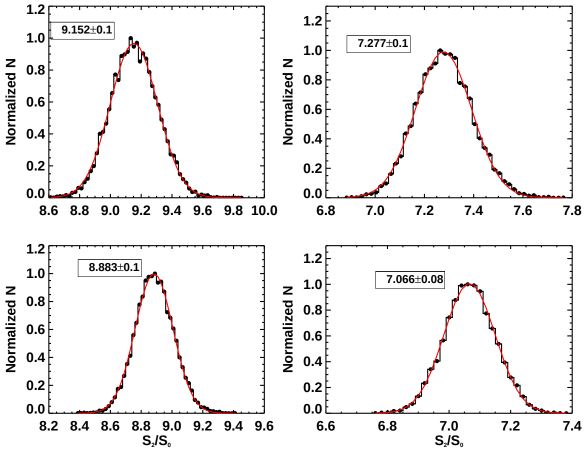

Figure 7. Distribution of S_2/S_0 ratio for 10^5 Monte Carlo iterations in histograms. Solid red lines denote Gaussian fit to the resulting distributions.

Results of the plane-fitting procedure have been listed in Table 2. Errors in i and $\theta_{\rm lon}$ were obtained from the propagation of error formula. From Table 2, one can find that the values of i are comparable to each other within the error bars indicating that the values obtained using two different datasets and empirical relations are reliable. On the other hand, if we compare the values of viewing angle parameters, then we find that $\theta_{\rm lon}$ values of the SMC main body are significantly different for the two bands. Difference in the $\theta_{\rm lon}$ arises due to poor sampling in distance distribution in the case of V-band as compared to those in the I-band. We take the results obtained from the I-band data to be more reliable because of larger number of stars and better phase coverage of light curves as compared to the corresponding V-band light curves. The viewing angle parameters obtained for NE arm of the SMC indicate that it is slightly misaligned with the SMC main body. Cumulative distribution of extinction corrected magnitudes (V_0) and metallicities $([Fe/H])$ of NE arm (sample 1) and SMC main body (sample 2) are shown in Fig. 9. In order to test whether the two samples came from the same distribution at a significance level of 0.05, we use two sample Kolomogorov-Smirnov (KS) statistics (Press et al. 2002). The KS statistics looks at the maximum absolute difference between the empirical CDF of sample 1 and empirical CDF of sample 2. It is a nonparametric test that allows statistical comparison of two one-dimensional distributions. The KS test applied to the two samples yields D-value and P-value. Here, D is the maximum value of the absolute difference between the two CDFs. From Fig. 9, one can find that since the P-value is greater than our assumed significance level of 0.05, we reject the null hypothesis and conclude that the cumulative distribution of sample 1 is significantly different from sample 2, with sample 1 being brighter and metal rich as compared to sample 2. Application of planefit procedure to the V-band data directly with distance determined using the MVF and MVC methods yields the value of c in Eqn. 9 to be -5.949 ± 0.233 kpc and -8.087 ± 0.364 kpc, respectively. Corresponding values of c obtained from the I-band data calibrated to the V-band are -5.299 ± 0.509 kpc and

---

[3] `http://www.r-project.org/`

Table 1. Geometric parameters of the SMC determined from the OGLE III I- and V-band data using absolute magnitude values determined from the Fourier method and the relation given by Catelan & Cortés (2008).

			Geometric parameters				
		Method	$S_0/\overline{S_0}$	S_1/S_0	S_2/S_0	$i[°]$	$\theta_{\rm lon}[°]$
Band	I	MVF	1.000 ± 0.004	1.334 ± 0.007	08.884 ± 0.123	1.713 ± 0.128	74.063 ± 0.510
		MVC	1.000 ± 0.004	1.327 ± 0.008	09.153 ± 0.154	1.912 ± 0.136	73.913 ± 0.589
	V	MVF	1.000 ± 0.002	1.281 ± 0.006	07.067 ± 0.083	2.860 ± 0.136	72.848 ± 0.496
		MVC	1.000 ± 0.003	1.243 ± 0.008	07.278 ± 0.114	3.637 ± 0.171	72.516 ± 0.714

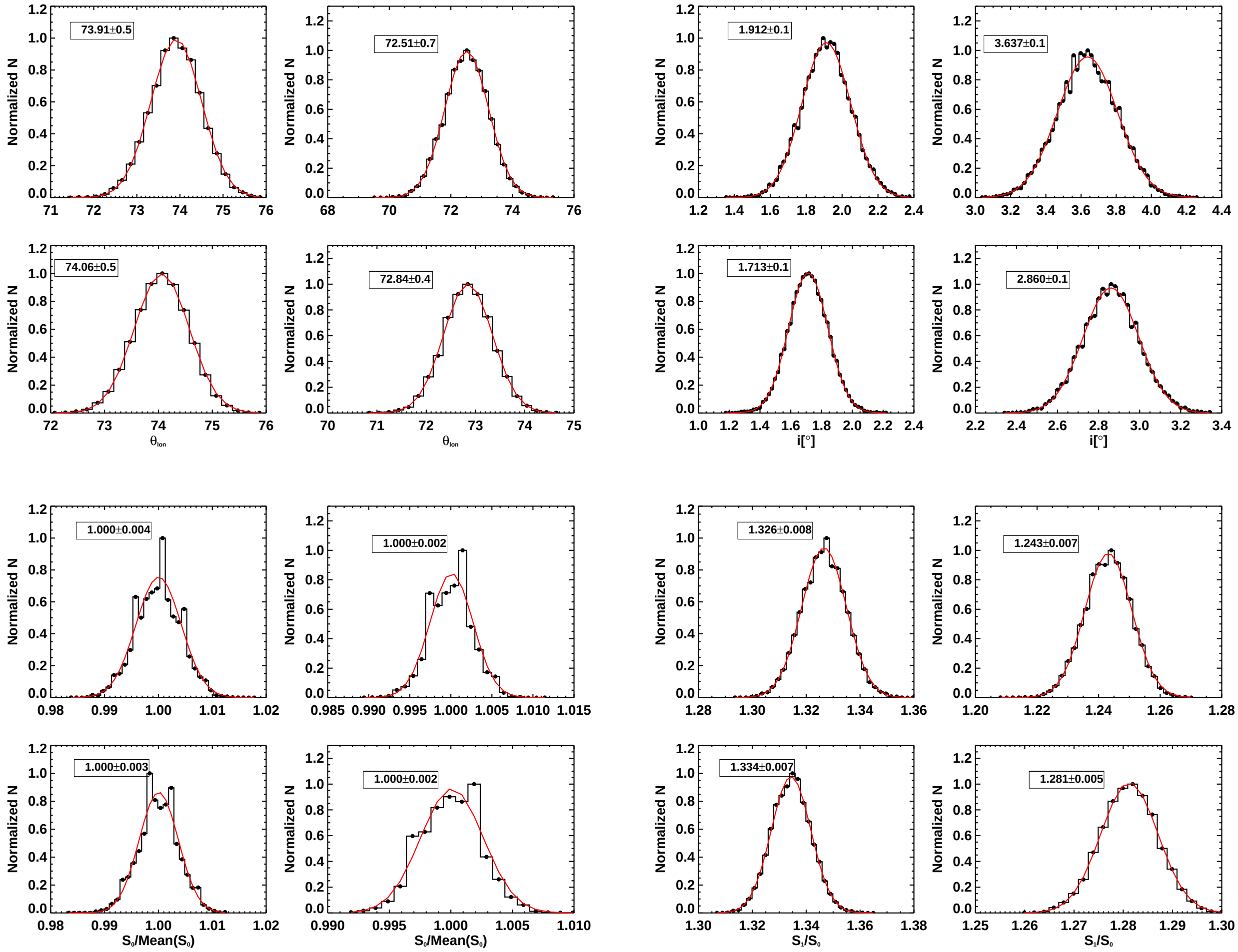

Figure 6. Distribution of viewing angles and geometrical parameters of the SMC in histograms. Solid red lines denote Gaussian fit to the resulting distributions.

-6.020 ± 0.847 kpc. Negative values of c obtained in each of the four cases indicate that NE arm of the SMC is nearer to us than the plane of the SMC main body. Since in majority of the cases, we get the NE arm to be nearer to us by ~ 6 kpc, we take this as the tentative estimate. It has also been found from the analyses that residuals of the planefit reveal a highly symmetric hyperbolic paraboloid warp of low amplitude ($\sim$ 0.03 kpc). In order to test whether the results obtained so far are an artifact or a real feature of the SMC, we resort to the metallicity relation of Smolec (2005) using I-band data directly and absolute magnitude relation of Catelan & Cortés (2008) as followed in section 9. Indeed, it has been found that same patterns are reflected and similar results are obtained in the resulting analyses.

7 LINE OF SIGHT DEPTH OF THE SMC

Line of sight (LOS) of the SMC has been studied using numerous tracers in the literature and is an important parameter to ascertain the extent of the SMC (Crowl et al. 2001; Subramanian & Subramaniam 2009, 2012; Kapakos & Hatzidimitriou 2012; Haschke et al. 2012).

Table 2. Geometric parameters of the SMC determined from the OGLE III I- and V-band data using absolute magnitude values determined from the Fourier method and the relation given by Catelan & Cortés (2008).

			Geometric parameters				
		Method	$S_0/\overline{S_0}$	S_1/S_0	S_2/S_0	$i[^\circ]$	$\theta_{\rm lon}[^\circ]$
SMC Main Body (Ellipsoid-fit)	I	MVF	1.000 ± 0.003	1.185 ± 0.004	09.764 ± 0.144	0.753 ± 0.093	55.569 ± 0.771
		MVC	1.000 ± 0.004	1.186 ± 0.005	09.916 ± 0.188	0.573 ± 0.106	55.552 ± 0.949
	V	MVF	1.000 ± 0.004	1.346 ± 0.007	10.221 ± 0.149	0.801 ± 0.106	82.799 ± 0.401
		MVC	1.000 ± 0.006	1.342 ± 0.009	10.839 ± 0.254	0.354 ± 0.106	83.068 ± 0.551
SMC NE Arm (Plane-fit)	I	MVF	–	–	–	2.254 ± 0.856	85.937 ± 14.030
		MVC	–	–	–	2.254 ± 0.864	85.932 ± 14.149
	V	MVF	–	–	–	1.284 ± 0.210	83.710 ± 09.309
		MVC	–	–	–	0.500 ± 0.193	78.744 ± 22.445

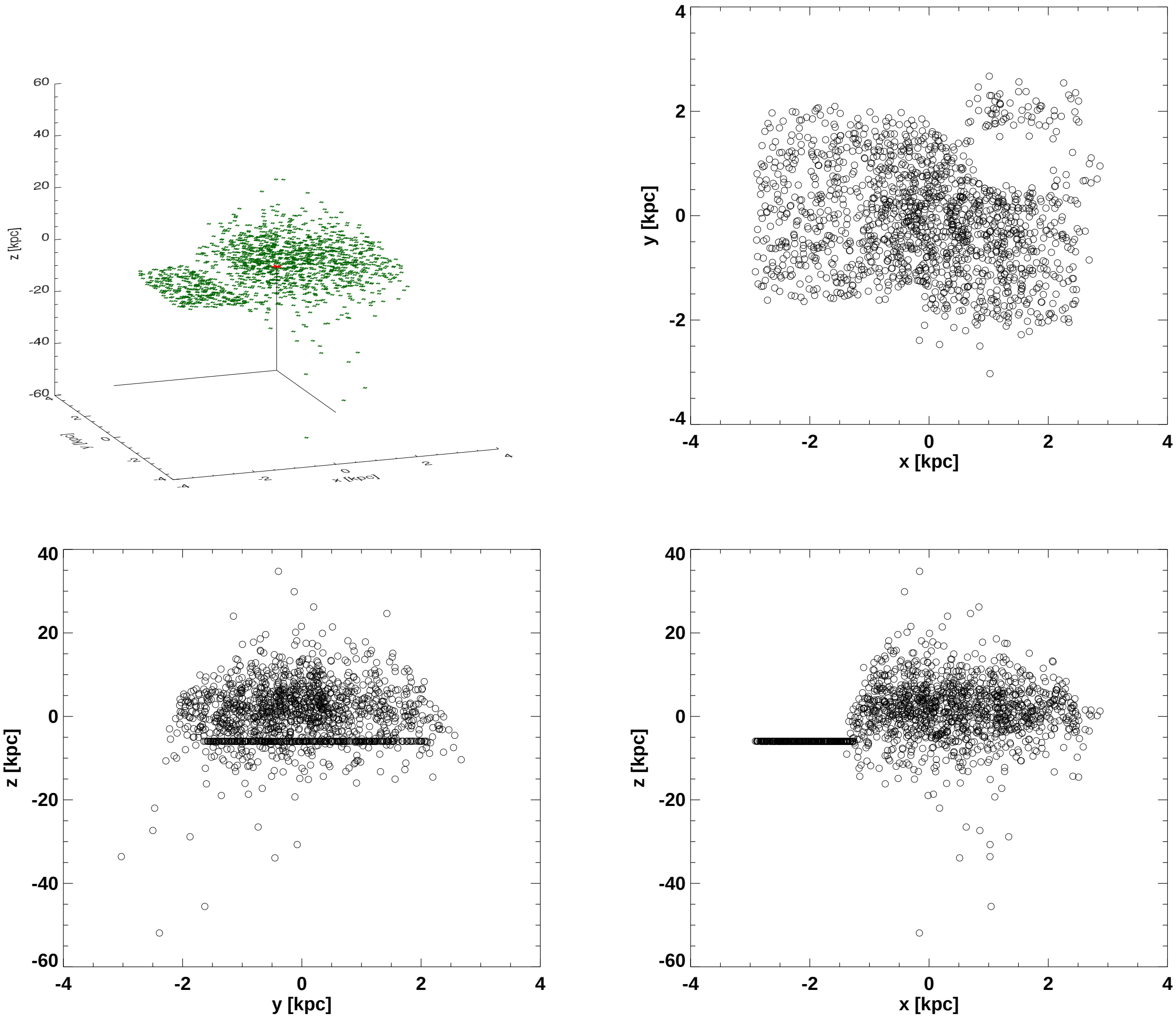

Figure 8. Upper left panel shows separation of SMC into its northeast arm (shown as planar distribution) and that of the main body (shown as ellipsoidal distribution). The centre of the galaxy is marked by red star symbol. Other panels depict the projected distributions on the XY, YZ and XZ planes as well. The NE arm appears as a line in the two-dimensional YZ and XZ projections.

RR Lyrae stars in the present analysis have been used as proxies to get an estimate of the LOS depth. When combined with the metallicity values, it serves as a robust parameter to the underlying different galactic substructures (Crowl et al. 2001; Kapakos & Hatzidimitriou 2012). To estimate the intrinsic line of sight depth of the SMC, we take into account the standard deviation ($\sigma_{\rm obs}$) distribution of the RRab distances and measurement errors ($\sigma_{\rm error}$) in the individual distances. The overall standard deviation ($\sigma_{\rm obs}$) is a combination of these two factors in quadrature (Crowl et al. 2001):

$$\sigma^2_{\rm obs} = \sigma^2_{\rm int} + \sigma^2_{\rm error}. \tag{10}$$

The intrinsic ±1σ line of sight depth is then given by $\left(\sigma^2_{\rm obs} - \sigma^2_{\rm error}\right)^2$. Using the I-band data, we have found the line of sight depth to be $1\sigma_{los} = 4.91 \pm 0.65, 4.12 \pm 0.71$ kpc from the distances determined using MVF and MVC, respectively. Corresponding values of these parameters in the V-band were found to be 5.34 ± 0.61 and 4.63 ± 0.83 kpc, respectively. From a study of 454 RRab stars in the V-band, Kapakos & Hatzidimitriou (2012) determined the LOS depth to be $\sigma_{int} = 5.3 \pm 0.4$ kpc. It may be noted that the LOS depth estimate has a lower value when Catelan & Cortés (2008) relation is used to derive the line of sight distances then when (Kovács & Walker 2001) relation is used. The variance weighted mean for the above estimates (weights $= \frac{1}{\sigma_2}$) yields $\sigma_{int} = 4.81 \pm 0.53$ kpc (Bevington & Robinson 2003). There is a caveat in the LOS depth estimation from the optical band photometric light curve data as it is highly sensitive to the interstellar reddenings. A large sample of near infrared (NIR) photometric light curve data can help us ascertaining the exact LOS depth of the SMC in different directions and thus help in locating the various components of the SMC. Use of different reddening maps applied to the optical band light curve data also yields different estimates of the LOS depth values (Crowl et al. 2001). However, most of the estimates of the 1σ LOS depth values are limited in the range between 4 and 6 kpc (Crowl et al. 2001; Subramanian & Subramaniam 2012; Haschke et al. 2012; Kapakos & Hatzidimitriou 2012). Despite completely different ways of obtaining the estimate of the LOS depth of the SMC from two OGLE bands, its value is consistent and well within the range. Combined with the LOS depth and the metallicity values of the sample, Kapakos & Hatzidimitriou (2012) found the existence of different structures consisting of different populations. Dividing the sample on the basis of their metallicities, they found that the metal rich stars show small variations in their LOS depth while the metal poor stars exhibit larger LOS depth variations. From their analysis, they also concluded that the inner regions of the SMC consists of a thicker structure mimicking a bulge. Metal rich and metal poor stars seem to belong to different dynamical structures. Metal poor stars have a smaller scale height and may belong to a thick disk and metal poor stars seem to belong to the halo. However, the results obtained by Kapakos & Hatzidimitriou (2012) should be taken with caution since these have been obtained from a smaller sample of 454 RRab stars with their V-band light curves and may suffer from selection effect. In order to test the results of Kapakos & Hatzidimitriou (2012), we have also investigated the LOS depth of the sample using the I-band data by dividing the sample into the metal poor ($[Fe/H] < \overline{[Fe/H]} - \sigma = -1.85$ dex) and metal rich stars ($[Fe/H] > \overline{[Fe/H]} + \sigma = -1.60$ dex). In order to find if there is any variation in the LOS depth of the two samples belonging to the different metallicity groups at a significance level of 0.05, we again perform a two sample KS test using the I-band data calibrated to the V-band. The two sample KS test yields $D = 0.110$ and P-value $= 0.90$. The P-value > 0.05 indicates that we fail to reject the null hypothesis implying that there is no evidence in the data to suggest that the two CDFs are different. This is contrary to that obtained by Kapakos & Hatzidimitriou (2012). While calculating the LOS depth, it has been found that observed uncertainties in the distance measurement ($\sigma_{\rm err}$) of a few stars are greater than the observed depth ($\sigma_{\rm obs}$). The LOS depth determinations for those stars have been left out.

To investigate the LOS depth variations in the SMC, we have divided the sample into three parts, viz., NE ($x < -0.5,\ y > 0.5$ kpc), central ($-0.5 < x < 0.5, -0.5 < y < 0.5$ kpc) and SW ($x > 0.5\ , y < -0.5$ kpc). In order to see the variation of depth among the three different regions of the SMC, we study their normalized LOS CDF distribution through KS test. A two sample KS test indicates that that LOS depth of the NE and SW parts of the SMC are not significantly different. On the other hand, KS test applied on LOS CDF distribution of the central part and other parts combined (NE+SW) yields $D = 0.316$ and P-value=0.008. These values indicate that the difference in CDF of the two distributions are different at a significance level of 0.05, with LOS depth of central part being larger than rest of the parts of the SMC. This indicates that SMC may have a bulge.

8 METALLICITY GRADIENT

The presence of radial metallicity gradient in a galaxy indicates the presence of different stellar populations which are responsible for formation and evolution of the galaxy (Bernard et al. 2008; Cioni 2009). The detection of metallicity gradient in the SMC using the CaII triplet (CaT) spectroscopy was first reported by Carrera et al. (2008) using the 350 red giant branch stars of 13 SMC fields distributed in the range $1^\circ - 4^\circ$ from the SMC center, wherein the metallicity decreases from the center of the galaxy towards the outermost regions. In their search for the metallicity gradient they also found that this gradient is related to an age gradient where the stars concentrated in the central regions are generally younger and metal rich. Recent studies attempt to bear out the presence of this gradient. Using the CaT metallicity study of the SMC field of 3037 red giant stars spread across 37.5 deg^2 centred on the galaxy, Dobbie et al. (2014) found evidence of metallicity gradient of -0.075 ± 0.011 dex/deg over the inner 5 deg suggesting an increasing number of young stars with decreasing galacto-centric radius. However, the formal errors in their determinations of $[Fe/H]$ are too optimistic. Finding meagre gradients as in the case of the SMC using the $[Fe/H]$ values requires careful estimations of their errors and determining the weighted mean metallicities and their errors while binning the galacto-centric radius. The weighted mean metallicities and the errors in each bin tells how statistically significant the gradient is. Using a sample of 454 RRab stars in V-band from the OGLE-III database, Kapakos & Hatzidimitriou (2012) found a metallicity gradient of -0.013 ± 0.007 dex/kpc with increasing

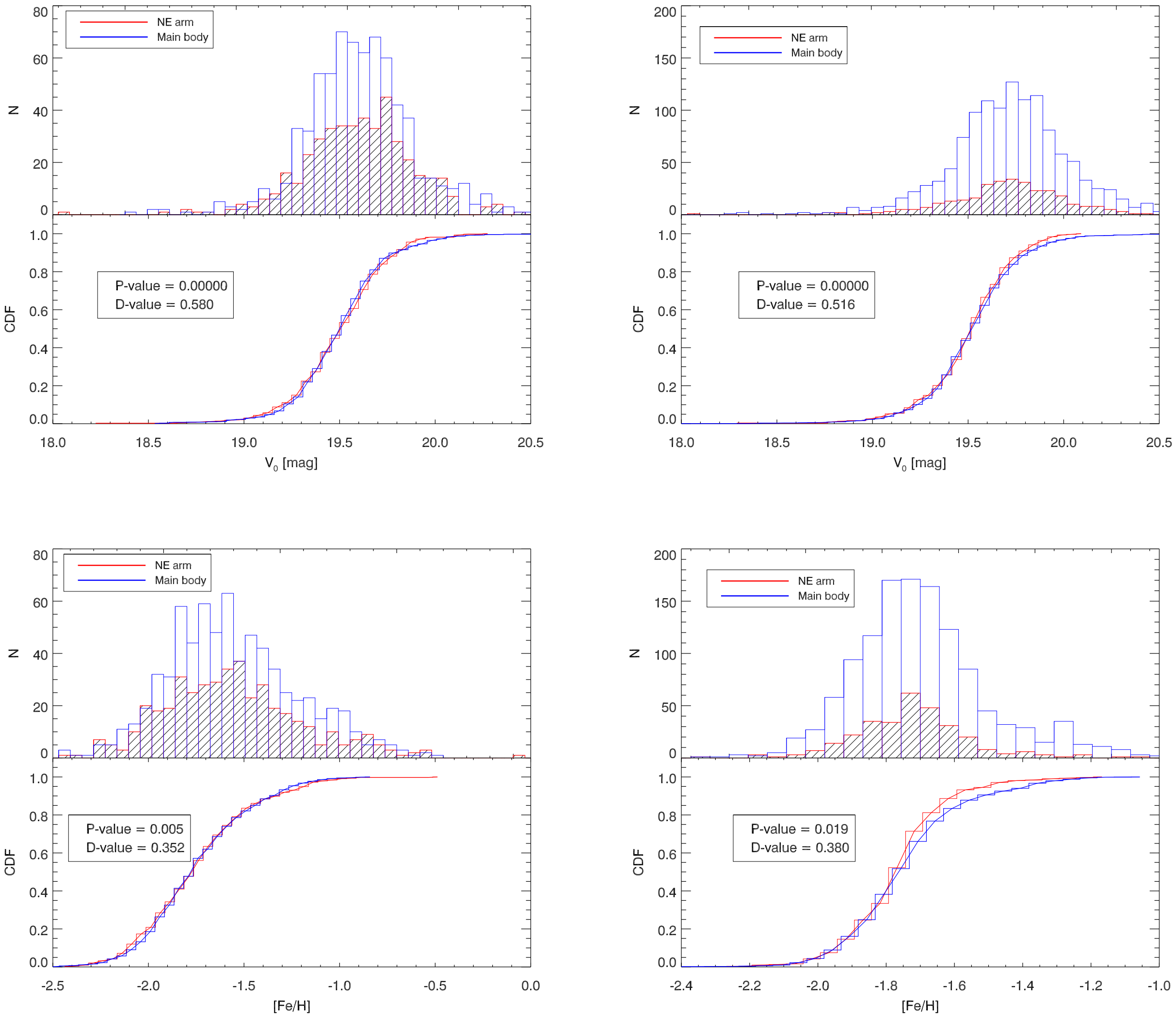

Figure 9. Cumulative distribution of extinction corrected RRab magnitudes V_0 and metallicities $[Fe/H]$ for the RRab stars (left panel shows the use of V-band directly on the empirical relation, whereas, right panel indicates the use of I-band data calibrated to the V-band). NE arm and SMC main bosy are marked with red and blue color lines, respectively.

metal abundance towards the dynamical center of the SMC. However, the contrary was found by Cioni (2009) using the $[Fe/H]$ derived from the ratio of C- and M-type AGB stars analysed as a function of galacto-centric distance. A constant value of $[Fe/H] = -1.25 \pm 0.01$ dex up to 12 kpc was obtained by Cioni (2009). The result of no metallicity gradient was reinforced by the study of the 25 SMC clusters on a homogeneous metallicity scale and with relative small metallicity errors by Parisi et al. (2009). Different values of metallcity gradients using various tracers obtained in the literature may be related to their redistributions from the positions they were formed (Roškar et al. 2008; Cioni 2009). Comparison of metallcities of SMC field and cluster stars similarly may also yield significant metallcity gradients due to the fact that the field stars are more metal poor than ther corresponding cluster stars surrounding them (Parisi et al. 2009).

In the investigation of any gradient in a galaxy, it is important to determine viewing angles of the galaxy accurately. In this paper, we have determined the geometry of the SMC using the more precise value obtained from the principal axis transformation applied on the de-projected Cartesian coordinates. In order to investigate for any metallicity gradient in the SMC, the true galacto-centric distances were obtained using the procedure described by Cioni (2009). The coordinate system was rotated according to

$$X' = X\cos(\theta) + Y\sin(\theta) \tag{11}$$
$$Y' = -X\sin(\theta) + Y\cos(\theta). \tag{12}$$

The $(X',\ Y')$ system was then de-projected using

$$Y'' = Y'/\cos(i) \tag{13}$$

The angular distances were then calculated and converted

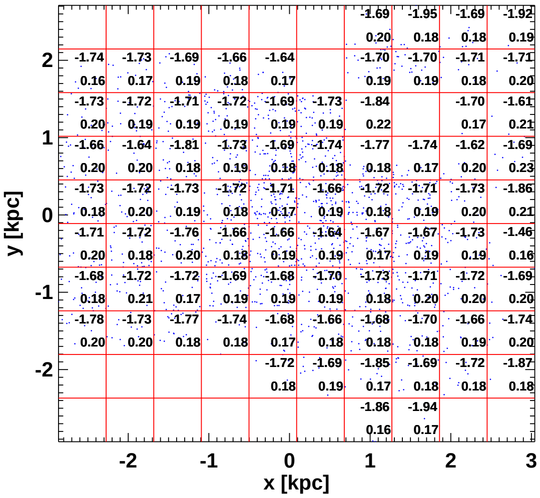

Figure 10. Metallicity distribution of RRab stars in the SMC. Metallicity values are binned on a 10 × 10 coordinate grid. In each bin, average metallicities and their associated errors are calculated which are due to uncertainties in the determination of Fourier parameter ϕ_{31} and are shown in each grid box.

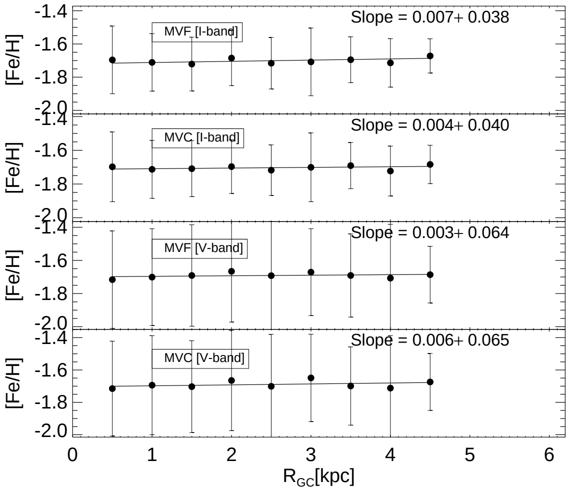

Figure 11. Mean metallicity distribution of RRab stars as a function of the galacto-centric distance (R_{GC}) in kpc with a bin size of 0.5 kpc. Mean metallicities in each bin have been obtained using the (Jurcsik & Kovacs 1996) empirical relations in the V and I-band with distances measured using the two methods described in the text.

into kpc with

$$d_{\rm deg} = \sqrt{X'^2 + Y''^2}, \tag{14}$$

$$d_{\rm kpc} = D \times \tan{(d)}, \tag{15}$$

where d is the angular distance to each star. Here the Cartesian coordinates $(X(\alpha,\delta), Y(\alpha,\delta))$ are calculated following the method described in van der Marel & Cioni (2001). This transformation helps in projecting a sphere onto a plane. Metallicity distribution of RRab stars in the SMC is shown in Fig. 10. Metallicity values are binned on a 10 × 10 coordinate grid. In each bin, the average metallicities and the associated errors which are due to the uncertainties in the determination of the Fourier parameter ϕ_{31} are calculated. Fig. 11 depicts the variance weighted mean metallicity values computed for four sets as a function of galacto-centric distance in bins of 0.5 kpc from the SMC center. A least-squares fit to the distance and mean metallicity values with their estimated errors to each of the data sets yields slopes of $0.007 \pm 0.038, 0.004 \pm 0.040$, 0.003 ± 0.064 and 0.006 ± 0.065 dex kpc^{-1}. All these values correspond to no statistically significant metallicity gradient. In the estimation of mean metallicity values in each distance bin, it has been ensured that the number of stars is greater than 10 for reliable statistics. Also, in the calculation of mean metallicity errors, the errors due to the uncertainties in the Fourier parameters and the systematic errors in each of the empirical relations have been taken into account. These two errors were added quadratically for each star in order to estimate the mean metallicity and its associated error in a distance bin. All of the empirical relations for metallicity calculations do not show any significant metallicity gradient within the uncertainties, consistent with the results obtained by Cioni (2009) and Parisi et al. (2009).

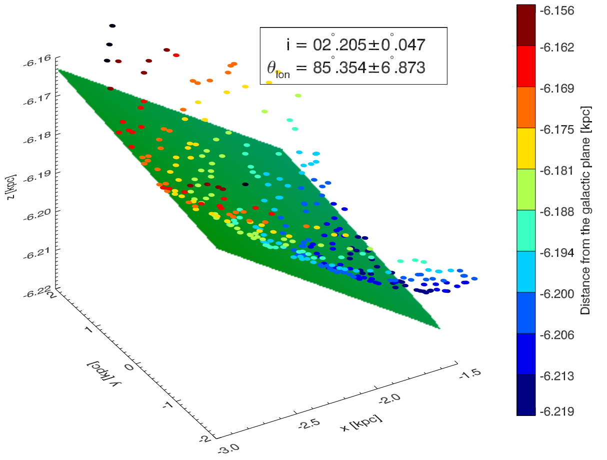

Figure 12. NE part of the SMC. Solid surface in green color denotes planefit to the data.

9 SMC STRUCTURE DETERMINATION USING SMOLEC'S (2005) METALLICITY RELATION

In order to compare, contrast and substantiate the viewing angle and geometrical structural parameter determinations of the SMC using V- and I-band data as discussed above, we now use the $M_V - [Fe/H]$ relation of Catelan & Cortés (2008) with $[Fe/H]$ determined from the I-band light curve data directly using the Smolec (2005) relation. Absolute magnitude determined using the Smolec (2005) relation is referred to as 'MVS'. The inclination angle and position angle of line of nodes for the entire sample of RRab stars obtained from the ellipsoid fitting were found to be $i = 3^\circ.144 \pm 0^\circ.129$ and $\theta_{\rm lon} = 74^\circ.856 \pm 0^\circ.514$. The axes ratios were obtained as: $1.000\pm0.002 : 1.284\pm0.006 : 7.474\pm0.101$. The sample of RRab stars are divided belonging to the SMC main body and NE arm on the basis of the changepoint analysis. Bimodal distribution of z-values also discriminates the NE arm from the main body of the SMC. A planefit procedure is applied to the NE arm which yields the value of $c = -6.251 \pm 0.854$ kpc. The fitted plane is shown in Fig. 12. The constant c represents the shift in the positive or negative z-direction from the xy-plane of the SMC. The value of c indicates that NE arm of the SMC is located at a distance ∼ 6 kpc below the plane of the SMC main body, hence making it nearer to us by ∼ 6 kpc than the main SMC plane. Several studies using Cepheids in the SMC found that the northeast arm of the SMC is nearer to us than the central bar (Caldwell & Coulson 1986; Mathewson et al. 1988; Sharpee et al. 2002). This study using statistically siginificant number of RRab stars further provides an insight into the issue thus confirming the previous findings. The viewing angle parameters for the NE arm are $i = 2^\circ.205 \pm 0^\circ.407$ and $\theta_{\rm lon} = 85^\circ.354 \pm 6^\circ.873$. Fig. (13) shows the residuals after the NE arm planefit values were subtracted from their corresponding z-values. A highly symmetric hyperbolic paraboloid warp of very low amplitude (∼ 0.03 kpc) in the residuals is clearly discernible. Tidal effects produced by the LMC (Large Magellanic Cloud) and the SMC main body may be attributed to this warp. Similarly, the ellipsoid fitting procedure is applied to the main body of the SMC which yields the values of $i = 0^\circ.178 \pm 0^\circ.091$ and $\theta_{\rm lon} = 57^\circ.053 \pm 0^\circ.644$ and axes ratios as $1.000\pm0.002 : 1.185\pm0.004 : 8.298\pm0.131$. The presence of metallicity gradient as a function of galacto-centric distance of the SMC is also investigated using the empirical relation of Smolec (2005) with galacto-centric radius determined from inclination and position angle values as obtained from the I-band data where distance is determined from the Catelan & Cortés (2008) empirical absolute magnitude relation. The gradient obtained is -0.008 ± 0.058 dex kpc^{-1}. This is similar to the gradient of 0.00 ± 0.06 dex kpc^{-1} obtained by Haschke et al. (2012) corroborating evidence of no gradient and is contrary to the value of -0.013 ± 0.007 dex kpc^{-1} obtained by Kapakos & Hatzidimitriou (2012) from the analysis of OGLE-III V-band light curves of 454 RRab stars. Fewer number of data points and poor phase coverage in the case of V-band light curves of OGLE-III as compared to the I-band light curves yield unreliable estimates of parameters determined using them and hence should be taken with caution. The data in the V-band also suffer from spatial resolution which might also result into poor estimates of viewing angles and geometric parameter determinations for the SMC. Fig. 14 shows cumulative distribution of extinction corrected RRab magnitudes V_0 for the RRab stars in the calibrated V-band as well as metallicities calculated using Smolec (2005) relation. The probability values obtained from the two sample KS tests applied on stars belonging to the NE arm (sample 1) and the SMC main body (sample 2) show that the CDFs of the two samples are significantly different at a level of 0.05 with sample 1 nearer to us and contains more metal rich stars as compared to sample 2, thus confirming the fact that the NE arm of the SMC is nearer to us and contains more metal rich stars. We have also investigated the LOS depth of the sample by dividing into the metal poor ($[Fe/H] < \overline{[Fe/H]} - \sigma = -1.96$ dex) and metal rich stars ($[Fe/H] > \overline{[Fe/H]} + \sigma = -1.58$ dex). In order to find if there is any variation in the LOS depth of the two samples belonging to different metallicity groups at a significance level of 0.05, we again perform a two sample KS test. The two sample KS test yields $D = 0.150$ and P-value $= 0.79$. The P-value > 0.05 indicates that we fail to reject the null hypothesis implying that there is no evidence in the data to suggest that the two CDFs are different. This supports the result by Haschke et al. (2012) that there are no variations in the LOS depth for different metallicity groups along the different SMC fields as observed by OGLE III photometric survey and is contrary to that obtained by Kapakos & Hatzidimitriou (2012). While calculating the LOS depth, it has been found that the observed uncertainties in the distance measurements ($\sigma_{\rm err}$) of a few stars are greater than the observed depth ($\sigma_{\rm obs}$). The LOS depth determinations for those stars have been left out. The mean LOS depth ($\overline{\rm LOS}$) of the SMC is found to be 4.31 ± 0.34 kpc. This value is in good agreement with the values of 4.13 ± 0.27 kpc, 4.07 ± 1.68 kpc and 4.2 ± 0.3 kpc found by Kapakos et al. (2011), Subramanian & Subramaniam (2012) and Haschke et al. (2012), respectively.

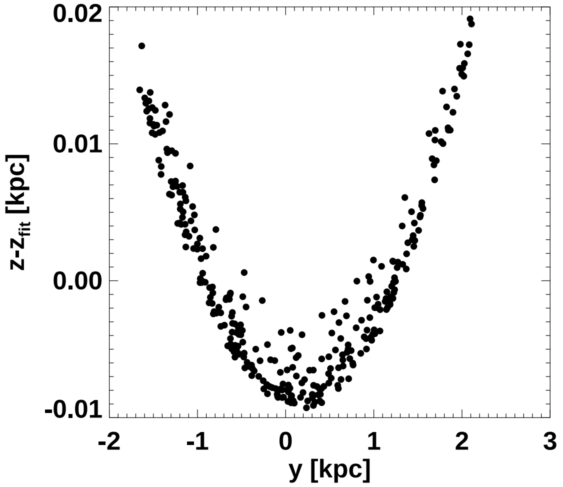

Figure 13. Distribution of residuals ($z - z_{\rm fit}$) of the NE arm RR Lyrae stars as a function of y coordinates, where $z_{\rm fit}$ are the fitted z-values obtained from Eqn. (9) . The distribution of stars take a hyperbolic paraboloid shape in 3d because of the gravitational interation exerted on it by the LMC and the main body of SMC. The scatter in the 2d plot is due to the projection from 3d.

In order to see the line of sight depth variations in the SMC, we have divided the sample into three parts, viz., NE ($x < -0.5,\ y > 0.5$ kpc), central ($-0.5 < x < 0.5, -0.5 < y < 0.5$ kpc) and SW ($x > 0.5\ , y < -0.5$ kpc). In order to see the variation of depth among the three different regions of the SMC, we study their normalized LOS CDF distribution through KS test. A two sample KS test indicates that that LOS depths of the NE and SW parts of the SMC are not significantly different. On the other hand, KS test applied on the LOS CDF distribution

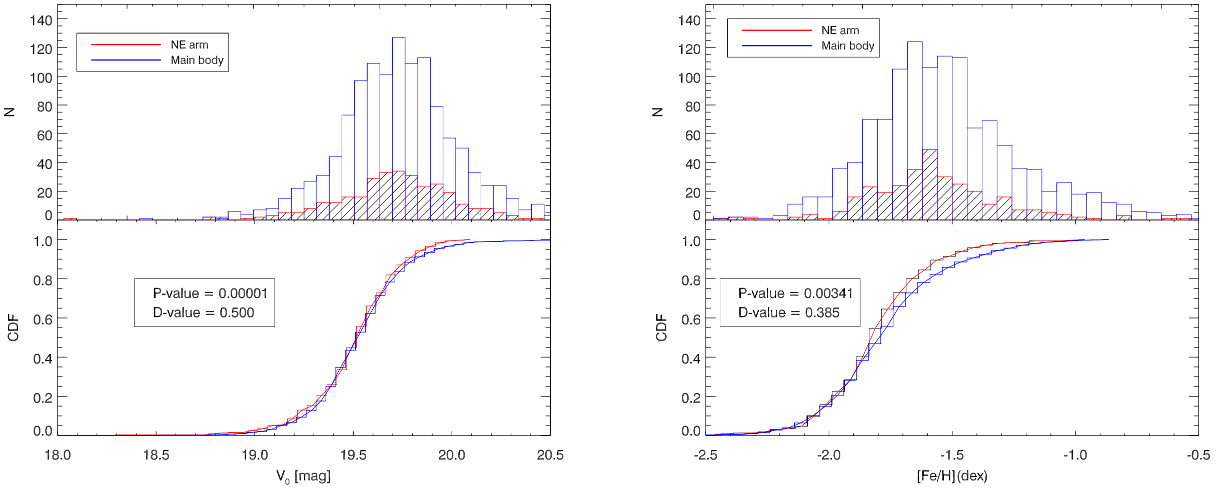

Figure 14. Cumulative distribution of extinction corrected RRab magnitudes V_0 for the RRab stars in the V-band with metallicities as determined from the (Smolec 2005) relation. Stars in the northeastern arm and the SMC main body are marked with red and blue color lines, respectively.

of the central part and other parts combined (NE+SW) yields $D = 0.40$ and P-value=0.002. These values indicate that CDF of the two distributions are different at a significance level of 0.05, LOS depth of the central part being larger than rest of parts of the SMC. This supports the findings of Subramanian & Subramaniam (2009) and Kapakos & Hatzidimitriou (2012) that the SMC may have a central bulge.

10 SCALE LENGTH AND TIDAL RADIUS OF THE SMC

Scale length is defined as the point where the number density of stars falls by a factor of $1/e$. Radial number density profiles of RRab stars are obtained by finding the radial number density of stars around the centroid of the galaxy in a given galacto-centric radius with increasing binsize of 0.5 kpc and is shown in Fig.15. The number density profile is modeled with an exponential disk to find the scale length. To find the extent of the SMC in the xy-plane, radial number density distribution is fitted with King's three parameter profile (King 1962). The tidal radius gives an estimate of full extent of the SMC in the xy-plane. King's three parameter profile is described by (King 1962)

$$n(r) = n(r_{0k})\left(\frac{1}{[1+(r/r_c)^2]^{\frac{1}{2}}} - \frac{1}{[1+(r_t/r_c)^2]^{\frac{1}{2}}}\right)^2. \quad (16)$$

The exponential disk profile is given by

$$n(r) = n(r_{0e})\exp(-\frac{r}{h}), \quad (17)$$

where $n(r_0)$ and h represent the density of RRab stars near the galactic center and scale length, respectively. r is the galacto-centric distance in kpc. r_t is called the tidal radius and represents the value of r at which $n(r)$ falls to zero and r_c is the core radius where the number density of stars falls to half its central value (King 1962). The various parameters obtained from modeling the radial density profile with exponential disk profile and three parameter King's profile are shown in Table 3. The variance weighted mean values were obtained as: $r_c = 0.73 \pm 0.02$ kpc, $r_t = 4.03 \pm 0.11$ kpc and $h = 1.84 \pm 0.04$ kpc. Although the values of h and r_c found here are comparable to the values of 1.87 ± 0.10 kpc and 1.082 ± 0.02 kpc, the value of $r_t = 4.03 \pm 0.11$ kpc is drastically different from the value of 7 ± 1 kpc obtained by Subramanian & Subramaniam (2012). Tidal radius is comparable to the 1σ LOS depth of ~ 4.00 kpc obtained in this analysis. This implies that extent of SMC in the xy-plane is comparable to the front-to-back distance along the line of sight and points to the possibility that RRab stars in the SMC are distributed more like a spheroid/slightly ellipsoid. The values of r_c and r_t imply that the concentration parameter defined as $c = \log(r_t/r_c)$ (King 1962) has a value $\sim 1.71 \pm 0.07$.

Table 3. Parameters of exponential and King's profiles for the radial number density distribution using the I-band data

Method	$n(r_{0e})$ (stars kpc^{-2})	$n(r_{0k})$ (stars kpc^{-2})	h (kpc)	r_c (kpc)	r_t (kpc)
MVF	844 ± 73	791 ± 62	1.89 ± 0.10	0.72 ± 0.10	3.91 ± 0.46
MVC	796 ± 69	746 ± 60	1.84 ± 0.09	0.72 ± 0.10	4.10 ± 0.49
MVS	755 ± 67	711 ± 58	1.81 ± 0.09	0.75 ± 0.11	4.11 ± 0.49

11 SUMMARY AND CONCLUSIONS

In this paper, we have studied both V and I-band light curves of RRab stars obtained from the OGLE-III project. Metallicities of RRab stars in the present sample were determined using the Jurcsik & Kovacs (1996) relation for both V and I-band data. Absolute magnitudes of the RRab stars were determined in both ways from the Fourier parameter

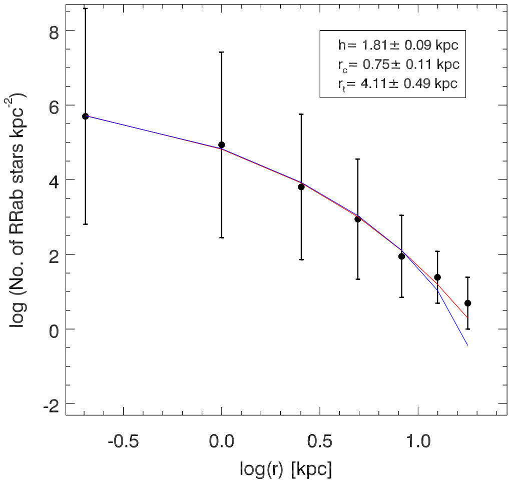

Figure 15. Radial density distribution of the RRab stars in he SMC is shown as black circles. Error bars are due to the Poissonian distribution ($\sigma \sim \sqrt{N}$). Red and blue solid lines show the model fits with the empirical two parameter exponential and three parameter density profiles (King 1962).

inter-relation of Kovács & Walker (2001) and those given by Catelan & Cortés (2008). Results of the above analysis were further substantiated using the I-band data with Smolec (2005) metallicity relation for the I-band and empirical $M_V - [Fe/H]$ relation of Catelan & Cortés (2008). Also, since the I-band light curve data have very good phase coverage, we adopt the final results obtained from the I-band data only. Based on the metallicity of RRab stars combined with their distance distributions in the SMC, the following conclusions are drawn:

(i) RR Lyrae stars in NE arm are nearer to us than the xy-plane of the SMC main body by a distance of ~ 6 kpc. Apart from that, the NE arm contains more metal rich stars as seen from metallicity distributions of these two groups using the two sample KS-statistics. Using the age, metal abundance and positional data of populous cluster using Cepheids in the SMC, Crowl et al. (2001) found that the eastern side of the SMC containing Cepheids is nearer to us and contains more metal rich stars but warrants further study. The investigation done in this study bears out this fact. The existence of an isolated NE arm of the SMC was further corroborated using the Schlegel et al. (1998) reddening map. However, it indicates that the NE arm is nearer to us by ~ 11 kpc than the galactic plane of the SMC main body. The Schlegel et al. (1998) maps use *IRAS* DIRBE data on the far-IR sky emission and estimate the extinction from the dust properties directly. Nonethless, the Schlegel maps are highly uncertain in the inner region of the SMC because their temperature structures were not sufficiently resolved by DIRBE (Schlegel et al. 1998; Pessev et al. 2006). The choice of different search radius as well as different reddening maps may have some effect on the final result of this paper. Availability of accurate and highly precise extinction measurements covering the entire region of the SMC will help enhance our understanding of its structure in great details.

(ii) Modeling the observed population of RRab stars in the SMC by a triaxial ellipsoid, we estimated the axes ratio, inclination of longest axis with the line of sight (i) and the position angle of line of nodes ($\theta_{\rm lon}$) on the sky from the analysis of the entire sample of RRab stars. Axes ratios of the galaxy were obtained as $1.00 \pm 0.000 : 1.310 \pm 0.029 : 8.269 \pm 0.934$ with $i = 2^\circ.265 \pm 0^\circ.784$, $\theta_{\rm lon} = 74^\circ.307 \pm 0^\circ.509$ from the variance weighted I-band determinations. Using the 12 populous clusters in the SMC, Crowl et al. (2001) obtained the axes ratios approximately as $1 : 2 : 4$ modeling the SMC as a triaxial galaxy with declination, right ascension and line of sight depth as the three axes. On the other hand, using the same OGLE-III SMC RRab dataset, Subramanian & Subramaniam (2012) obtained the axes ratios, inclination of the longest axis with the line of sight (i) and the position angle of the projection of the ellipsoid on the plane of the sky ($\theta_{\rm lon}$) as $1.00 : 1.30 : 6.47$, $0^\circ.4$, $74^\circ.4$, respectively, with no errors in the parameters quoted. Whereas, Haschke et al. (2012) found an inclination angle of $7^\circ \pm 15^\circ$ and a position angle of $83^\circ \pm 21^\circ$ from 1494 OGLE-III RR Lyrae stars using only the I-band data. These values are quite consistent with those obtained in the present study using distance distributions determined from the $M_V - [Fe/H]$ and M_V-Fourier parameters relations.

(iii) NE arm of the SMC resembles a three-dimensional plane with the plane slightly warped in a hyperbolic paraboloid, while the the SMC main body is distributed like an ellipsoid. The NE arm has been fitted by a plane equation to determine its viewing angles. The SMC main body has been fitted with an ellipsoid obtained from the principal axis transformation of the moment of inertia tensor constructed from the (x, y, z) coordinates. Analyses indicate that the NE arm is slightly misaligned with the SMC main body, with a highly symmetric warp of low amplitude (~ 0.03 kpc). The warp may have been caused by the tidal forces exerted on it by the main SMC body and the LMC. Axes ratios of the SMC main body were obtained as $1.00 \pm 0.000 : 1.185 \pm 0.001 : 9.411 \pm 0.860$ with $i = 0^\circ.507 \pm 0^\circ.287$, $\theta_{\rm lon} = 55^\circ.966 \pm 0^\circ.814$ from the variance weighted I-band determinations. On the other hand, viewing angle parameters of the NE arm are found to be $i = 2^\circ.244 \pm 0^\circ.024$ and $\theta_{\rm lon} = 85^\circ.541 \pm 0^\circ.332$ from the variance weighted I-band determinations.

(iv) Combining metallicities with spatial distribution of these tracers, no radial metallicity gradient in the SMC has been detected. Dividing the entire sample into three parts: northeastern (NE), central and southwestern (SW), we found that the central part has a significantly larger line of sight depth as compared to rest of the parts, indicating that the SMC may have a bulge. Independent analysis done in this work exploring different empirical relations and photometric bands provides substantial evidence to the findings of Subramanian & Subramaniam (2009) and Kapakos & Hatzidimitriou (2012) of SMC having a central bulge.

(v) Radial number density of RRab stars in the I-band were modeled by an exponential disk and three parameter King (1962) profiles. Following values were obtained from the modeling: $h = 1.84 \pm 0.04$ kpc, $r_c = 0.73 \pm 0.02$ kpc, $r_t = 4.03 \pm 0.11$ kpc and $c = 1.71 \pm 0.07$.

ACKNOWLEDGMENTS

The authors thank the OGLE team for making their invaluable variable star data publicly available. SD thanks Department of Science & Technology (DST), Govt. of India for support through a research grant D.O No. SB/FTP/PS-029/2013 under the Fast Track Scheme for Young Scientists. HPS and SMK acknowledge Indo-US Science & Technology Forum (IUSSTF) for support. SD and SK also acknowledge support through funding in the DU innovation scheme by University of Delhi. The authors acknowledge helpful discussions with Chow Choong Ngeow on extinction determinations. The use of arxiv.org/archive/astro-ph and NASA ADS databases is highly acknowledged. The authors thank the anonymous referee for all the insightful comments and suggestions that significantly improved the paper.

REFERENCES

Alcock C., Allsman R. A., Alves D. R., Axelrod T. S., Basu A., Becker A. C., Bennett D. P., Cook K. H., Drake A. J., Freeman K. C., Geha M., Griest K., King L., Lehner M. J., Marshall S. L., Minniti D. a., 2000, AJ, 119, 2194

Arellano Ferro A., Giridhar S., Bramich D. M., 2010, MNRAS, 402, 226

Bernard E. J., Gallart C., Monelli M., Aparicio A., Cassisi S., Skillman E. D., Stetson P. B., Cole A. A., Drozdovsky I., Hidalgo S. L., Mateo M., Tolstoy E., 2008, ApJ, 678, L21

Bevington P., Robinson D., 2003, Data reduction and error analysis for the physical sciences. McGraw-Hill Higher Education, McGraw-Hill

Caldwell J. A. R., Coulson I. M., 1985, MNRAS, 212, 879

Caldwell J. A. R., Coulson I. M., 1986, MNRAS, 218, 223

Carrera R., Gallart C., Aparicio A., Costa E., Méndez R. A., Noël N. E. D., 2008, AJ, 136, 1039

Catelan M., Cortés C., 2008, ApJ, 676, L135

Cioni M.-R. L., 2009, A&A, 506, 1137

Crowl H. H., Sarajedini A., Piatti A. E., Geisler D., Bica E., Clariá J. J., Santos Jr. J. F. C., 2001, AJ, 122, 220

Deb S., Singh H. P., 2009, A&A, 507, 1729

Deb S., Singh H. P., 2010, MNRAS, 402, 691

Deb S., Singh H. P., 2014, MNRAS, 438, 2440

Dobbie P. D., Cole A. A., Subramaniam A., Keller S., 2014, ArXiv e-prints

Graczyk D., Pietrzyński G., Thompson I. B., Gieren W., Pilecki B., Konorski P., Udalski A., Soszyński I., Villanova S., Górski M., Suchomska K., Karczmarek P., Kudritzki R.-P., Bresolin F., Gallenne A., 2014, ApJ, 780, 59

Groenewegen M. A. T., 2000, A&A, 363, 901

Haschke R., Grebel E. K., Duffau S., 2011, AJ, 141, 158

Haschke R., Grebel E. K., Duffau S., 2012, AJ, 144, 107

Haschke R., Grebel E. K., Duffau S., Jin S., 2012, AJ, 143, 48

Jeon Y.-B., Ngeow C.-C., Nemec J. M., 2014, in Guzik J. A., Chaplin W. J., Handler G., Pigulski A., eds, IAU Symposium Vol. 301 of IAU Symposium, Ground-based photometry for 42 Kepler-field RR Lyrae stars. pp 427–428

Jurcsik J., 1995, Acta Astronomica, 45, 653

Jurcsik J., Kovacs G., 1996, A&A, 312, 111

Kapakos E., Hatzidimitriou D., 2012, MNRAS, 426, 2063

Kapakos E., Hatzidimitriou D., Soszyński I., 2011, MNRAS, 415, 1366

Killick R., Eckley I., Haynes K., 2014, changepoint: An R package for changepoint analysis

Killick R., Eckley I. A., 2014, Journal of Statistical Software, 58, 1

King I., 1962, AJ, 67, 471

Kovács G., Walker A. R., 2001, A&A, 371, 579

Kunkel W. E., Demers S., Irwin M. J., 2000, AJ, 119, 2789

Markwardt C., , 2012, MPFIT: Robust non-linear least squares curve fitting

Markwardt C. B., 2009, in Bohlender D. A., Durand D., Dowler P., eds, Astronomical Data Analysis Software and Systems XVIII Vol. 411 of Astronomical Society of the Pacific Conference Series, Non-linear Least-squares Fitting in IDL with MPFIT. p. 251

Mathewson D. S., Ford V. L., Visvanathan N., 1988, ApJ, 333, 617

Nemec J. M., Cohen J. G., Ripepi V., Derekas A., Moskalik P., Sesar B., Chadid M., Bruntt H., 2013, ApJ, 773, 181

Nemec J. M., Smolec R., Benko J. M., Moskalik P., Kolenberg K., Szabo R., Kurtz D. W., Bryson S., Guggenberger E., Chadid M., Jeon Y.-B., Kunder A., Layden A. C., Kinemuchi K., Kiss L. L., 2011, MNRAS, 417, 1022

Nikolaev S., Drake A. J., Keller S. C., Cook K. H., Dalal N., Griest K., Welch D. L., Kanbur S. M., 2004, ApJ, 601, 260

Parisi M. C., Grocholski A. J., Geisler D., Sarajedini A., Clariá J. J., 2009, AJ, 138, 517

Pejcha O., Stanek K. Z., 2009, ApJ, 704, 1730

Pessev P. M., Goudfrooij P., Puzia T. H., Chandar R., 2006, AJ, 132, 781

Pietrzynski G., Thompson I. B., Gieren W., Graczyk D., Stcepien K., Bono G., Moroni P. G. P., Pilecki B., Udalski A., Soszynski I., Preston G. W., Nardetto N., McWilliam A., Roederer I. U., Gorski M., Konorski P., Storm J., 2012, NATURE, 484, 75

Pietrzyski G., Graczyk D., Gieren W., Thompson I. B., Pilecki B., Udalski A., Soszyski I., Kozlowski S., Konorski P., Suchomska K., Bono G., Moroni P. G. P., Villanova S., 2013, NATURE, 495, 76

Press W. H., Teukolsky S. A., Vetterling W. T., Flannery B. P., 2002, Numerical recipes in C++ : the art of scientific computing

Pritzl B. J., Olszewski E. W., Saha A., Venn K. A., Skillman E. D., 2011, AJ, 142, 198

Putman M. E., Gibson B. K., Staveley-Smith L., Banks G., Barnes D. G., Bhatal R., Disney M. J., Ekers R. D., Freeman K. C., Haynes R. F., Henning P., Jerjen H., Kilborn V., Koribalski B., Knezek P., 1998, NATURE, 394, 752

Roškar R., Debattista V. P., Stinson G. S., Quinn T. R., Kaufmann T., Wadsley J., 2008, ApJ, 675, L65

Sandage A., 2004, AJ, 128, 858

Schlegel D. J., Finkbeiner D. P., Davis M., 1998, ApJ, 500, 525

Sharpee B., Stark M., Pritzl B., Smith H., Silbermann N.,

Wilhelm R., Walker A., 2002, AJ, 123, 3216
Simon N. R., 1988, ApJ, 328, 747
Smith H. A., 2004, RR Lyrae Stars
Smolec R., 2005, Acta Astron., 55, 59
Soszyński I., Udalski A., Szymański M. K., Kubiak M., Pietrzyński G., Wyrzykowski Ł., Szewczyk O., Ulaczyk K., Poleski R., 2009, Acta Astron., 59, 1
Stanimirovic S., Staveley-Smith L., Dickey J. M., Sault R. J., Snowden S. L., 1999, MNRAS, 302, 417
Stanimirović S., Staveley-Smith L., Jones P. A., 2004, ApJ, 604, 176
Subramanian S., Subramaniam A., 2009, A&A, 496, 399
Subramanian S., Subramaniam A., 2012, ApJ, 744, 128
Subramanian S., Subramaniam A., 2014, ArXiv e-prints
van der Marel R. P., Cioni M.-R. L., 2001, AJ, 122, 1807
Weinberg M. D., Nikolaev S., 2001, ApJ, 548, 712
Westerlund B. E., 1997, The Magellanic Clouds
Zaritsky D., 1999, AJ, 118, 2824
Zaritsky D., Harris J., Thompson I. B., Grebel E. K., Massey P., 2002, AJ, 123, 855
Zinn R., West M. J., 1984, ApJS, 55, 45